The Efficiency of Perceptual Quality Metrics 3D Meshes Based on the Human Visual System

Nessrine Elloumi(✉), Habiba Loukil Hadj Kacem, and Med Salim Bouhlel

Research Unit: Sciences and Technologies of Image and Telecommunications, Higher Institute of Biotechnology, University of Sfax, Sfax, Tunisia
elloumi nessrine@gmail.com, loukil_habiba@net-c.com, medsalim.bouhlel@enis.rnu.tn

Abstract. The representation of content as a 3D mesh is a very emerging technology. These three-dimensional meshes can be a scan of objects, characters or 3D scenes. Mesh quality is a determining factor in treatment of effectiveness, accuracy of results and rendering quality. You can show users these 3D meshes with a texture on the 3D mesh surface. The estimated quality by an observer is a very complex task related to the complexity of the Human Visual System (HVS). In this paper we present the efficiency of perceptual quality metrics 3D meshes based on the human visual system.

Keywords: Perceptual quality · 3D metric · 3D meshes · HVS

1 Introduction

For several years, researchers in image [1] processing and computer graphics have worked on the definition of an effective objective metric, able to predict the perceived quality of images, videos and 3D scenes [2]. To design such a system, it was necessary to study and determine the structures of visual content. This task is more complex when we look at 3D content represented in the form of triangular meshes.

These 3D meshes are generally discrete packets of a non- uniform way to represent objects and scenes. Also, many operation can be performed on this 3D meshes [3], for example If we want to protect the 3D content we can use watermarking mesh algorithms for security purposes. It is also possible to apply a compression scheme to transmit on a low bandwidth network [4, 5] to reduce the size of 3D meshes [6]. Other operations on 3D meshes can be used, among which we mention: the quantification, enameling or deformation. These algorithms usually introduce inevitable distortion on the geometry sufaces mesh. It is therefore important to measure and evaluate the effect of these distortions that affect the quality triangular meshes.

2 The Perceptual Quality 3D Meshes

The study of perceptual quality is an important task since most visual data are for a final human observer. Measuring the perceptual quality can be carried out using measurements made by observers (subjective measures) or measurements from

V.E. Balas et al. (eds.), *Soft Computing Applications*, Advances in Intelligent Systems and Computing 633, DOI 10.1007/978-3-319-62521-8_43

algorithmic processes (objective measures). For each observer, quality can have a different definition of personal criteria. The main objective of measuring the perceptual quality is to analyze the behavior of the HVS [7] and quantify the quality as perceived by observers [8]. Human Vision System is based on two mechanisms: low-level mechanisms that affect the biophysical structure of the sensory system and high-level mechanisms related to human cognitive system.

3 Objective Measures of Quality Meshes

The estimate of the perceptual quality is an important element in assessing the meshes quality after treatments. The objective of the perceptual quality metrics is to judge the quality of a mesh based on human perception characteristics [9]. To do this, there are different approaches the top-down approach considers the HVS as a black box and tries to imitate the behavior of the system from the perspective of inputs/outputs and the bottom-up approach based on simulation and imitation of each component of HVS. To develop a 3D metrics [10], researchers can use two alternatives: either they use existing metrics of perceptual quality 2D images [11–13] on two-dimensional projections of 3D meshes (metric-based images and videos) or they use develop metrics based-models that exploit the term mesh geometry and connectivity signal to evaluate the quality [14]. To estimate the quality of 3D meshes, other classification of the quality metrics is possible.

*** Metrics "Full – Reference":** The original model is available in full, in which case we will try to quantify the existing difference between the original image and the degraded version.

*** Metrics to "Reduced Reference":** The original image is available in its entirety, but is represented by a vector containing a reduced set of attributes. In this case, an attempt to quantify the difference existing between the vectors associated to the original image and the vector resulting from a distorted version.

*** Metrics "No – Reference":** The original image is not available. In this case, it is possible to work with a priori on the degradation types that may be encountered, or, conversely, by making no assumption about possible distortions. Many of these metrics exploit the proprieties of the human visual system. To compare two 2D images or 3D meshes, it is common to use the signal to noise ratio measurements or geometric distances. These geometrical measurements do not include the properties of human vision system. From the literature it is approved that the metric based on the HVS are more appropriate than others [15].

4 The Human Visual System

The human visual system is a complex sensory system and not yet fully mastered. Nevertheless, it may be considered an information transcription system turned into usable data by the brain (Fig. 1). A conversion step can capture the received information and decoded into signals by the brain.

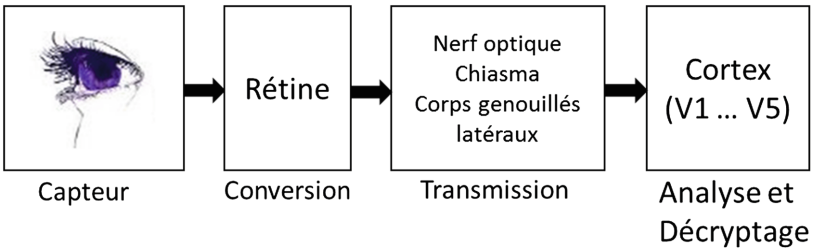

Fig. 1. Human visual system: simplified

It is the role of the eye that converts light energy into sensory signals and then transmits them to the visual cortex via the optic nerves and geniculate nucleus. The visual cortex decrypts and processes the information. To better understand the flow of information and operation of the HVS, we recall the essential elements that are involved in the process of gathering and processing of visual information (Capture, conversion, transmission and processing of information).

4.1 Sensor

- **The eye:** Which an optical system whose primary role is to converge the light signals to the conversion zone and transmit the decoded form in the brain. It comprises several important elements including:
- **The cornea:** is a convex spherical surface which separated the eye from the external environment. Its primary role is to focus the light rays received to the retina.
- **Iris:** Adapts the light intensity by varying its opening. So acts as an optical diaphragm.
- **The crystalline:** Allows to redirect the light flow to the retina where it's arranged into photoreceptor cells (Cones and rods). It plays the role of variable focus lens.

4.2 Conversion

- **The retina:** It converts the light signal captured by the receiving photocells into electrical signals which are then transmitted to the visual cortex via the optic nerve.
- **The retina:** is composed essentially of two types of receptors.
- **Cones:** Which are responsive to detail.
- **Rods:** Which are sensitive to low luminance (blurred vision and course) and intervene rather at night vision (monochrome).

4.3 Transmission

- **The optic nerve:** it transports information from the retina to the visual cortex, through the chiasm and lateral geniculation body.

– **The chiasm:** the direction Information goes through from the right eye and the left eye, chiasm's role is to transmit the information received to the lateral geniculation body.

4.4 Analysis and Decryption

– **The visual cortex:** His major role is the decrypting (or decoding) and the analyzing of the received signals.

5 The Human Visual System and the Perception of Visual Quality

Most of the existing metrics follow the approach Top – Down to study the human visual system and imitate its behavior.

The existing metrics has for objective to maximize the correlation of the results (profits) of prediction with the subjective scores. The subjective evaluation of the meshing quality is established by means of observers through psychometric experiments. Many databases were developed to have measures of the real structure of the 3D meshes perceptual quality. There are two important properties of the HVS that we have to consider in order to measure the perceptual quality of the 3D meshing [16].

5.1 Contrast Sensitivity Function

The function of spatial contrast sensitivity (notes CSF) models the sensitivity of the human visual system to spatial frequencies of the visual stimulus. The first Research Campbell - Robson on CSF have shown that Works with the HVS selectivity on spatial frequencies, sensitivity achieved its Maximum Value around four cycles per degree of visual angle [17].

Figure 2(a) shows that the pixel intensity is modulated by a horizontal sine function. When the spatial frequency of the pixel increases in a logarithmical way (on the horizontal axis), the contrast increases from top to bottom. Although the change contrast is the same for all frequencies, we observe that the bars appear to be highest in the middle of the image following the shape of the sensitivity function in Fig. 2(b). This effect is not made by the image, it's rather made by the property of frequency selectivity of the human vision system.

In the context of dynamic visual content (2D videos, dynamic meshes, etc.), the CSF must be modulated by stimuli speed. This is due to the variability of the contrast sensitivity depending on the speed of the stimulus movement. Since 1977, Kelly has presented an experimental study for modulating the function of contrast sensitivity affected by the test conditions (see Fig. 3(a)). In 1998, Daly has developed a dynamic model of CSF through a time function of CSF tends to move to lower frequencies. These studies were performed for achromatic data. Other studies have integrated color effect on the CSF: The contrast sensitivity (Fig. 3(b)). With increasing speed, the CSF

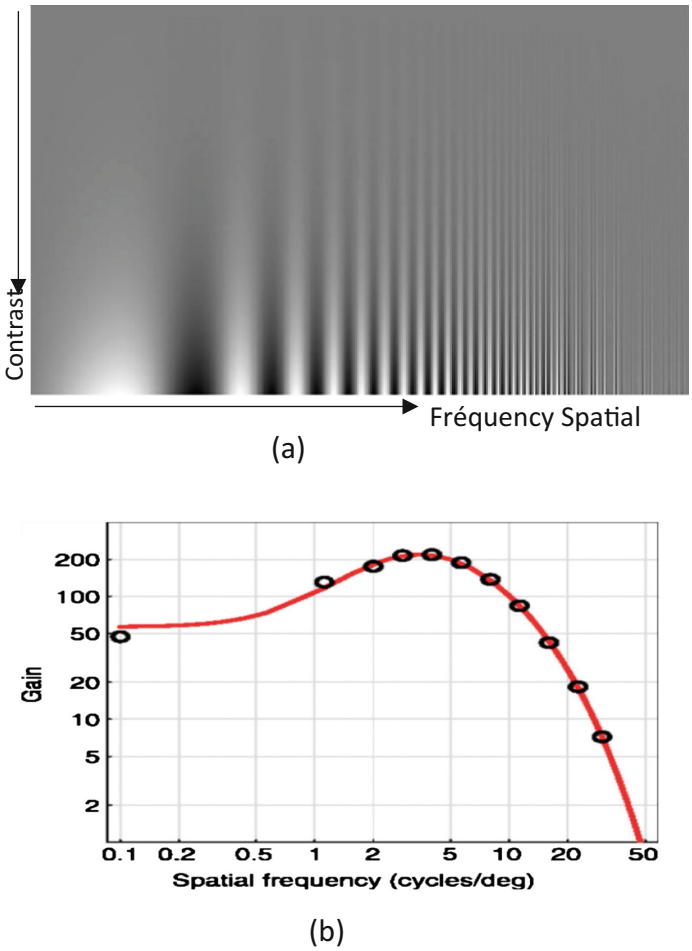

Fig. 2. The spectral properties of the HVS: (A) - graph illustrating Campbell- Robson contrast sensitivity (CSF), (b) - curve of HVS sensitivity as a function of spatial frequency.

curve tends to shift towards low frequencies. These studies were realized to achromatic data [18].

5.2 The Masking Effect

Masking is the effect of modification of the component bordures visibility in a multi-media content (masked signal) by the presence of another component (masking signal). The magnitude of this effect is measured by the change of the masked signal visibility with or without the presence of the masking signal [19]. Masking may intervene in the same frequency band (in-band masking) or between different frequency bands (inter-band masking). This type of mask in literature, called the entropy masking effect [20]. There is another type of contrast masking named masking contrast connected to the

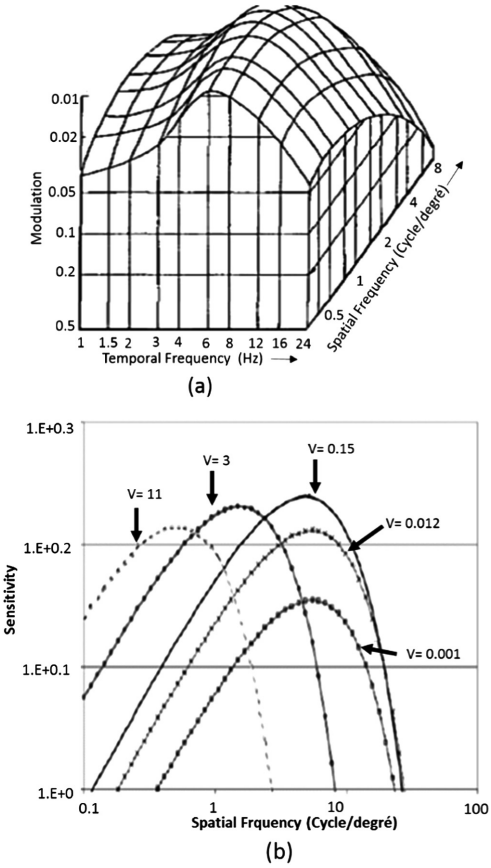

Fig. 3. Kelly Illustration (a) - for the presentation of the combination of the effect of spatial and temporal frequency on contrast sensitivity, and (b) - the CSF illustration depending on the speed. The time function of CSF in (b) is calculated from an empirical equation. The speeds V are measured in degree/second.

change of the surface visibility as a function of the contrast values. The spatial masking effect is often linked to the concept of surface roughness for 3D meshes [21].

5.3 The Perceptual Quality 3D Mesh

To measure the distance between two 3D meshes [22] many 3D metrics exist. We represent in the following sheet, the perceptual metrics developed for 3D meshes [23].

5.3.1 The 3D Watermarking Perception Metric

Corsini et al. have developed a new metric of quality [24]. Their approach, called 3DWPM (3D Watermarking Perception Metric), is based on the calculation of the perceptual distance between two meshes resting on surface roughness. This measured 3DWPM distance between two meshes M_1 and M_2 are identified by:

$$3\mathrm{DWPM}(\mathrm{M1},\mathrm{M2}) = \log\left(\frac{\rho(M2-\rho(M1)}{\rho(M1)} + K\right) - \log(\mathrm{k}) \tag{1}$$

where $\rho(\mathrm{M}_1)$ and $\rho(\mathrm{M}_2)$ measure the overall roughness of the two meshes and k is a constant varied digital. Two variants of 3DWPM were developed using descriptors of roughness differences. The first descriptor of roughness is used to 3DWPM1, is inspired by that of Lavoué [25]. The roughness measurement is calculated through measuring the dihedral angles between the normal facets in vicinity. The normal facet of a smooth surface does not vary greatly. In contrast, on textured regions (rough) these normal vary more significantly. A Multi - scale analysis of these entities is considered [26] to evaluate dihedral angles using the direct vicinity (1 ring) and the extended vicinity (1 ring, 2 rings, etc.). The second roughness measurement adopted by Corsini et al. is 3DWPM2, it is based on estimating of the roughness of surfaces by Wang et al. [27]. Their approach is based on the comparison of a mesh and smoothed versions of the same mesh. Smooth regions correspond to small differences while the rough areas have more significant differences.

5.3.2 The Mesh Structural Distortion Measure Metric

The MSDM (Mesh Structural Distortion Measure) uses the amplitude of the average curvature of the 3D mesh surface to quantify the perceptual distortion. This metric has been improved recently under the name MSDM2 by integrating multi-scale analyses [25]. In 2006, Lavoué et al. have introduced a structured distortion measurement called Structural Mesh Distortion Measure (MSDM) [28]. This quality measure was inspired by the quality measurement of 2D pictures SSIM (Structural SIMilarity index) introduced by Corsini et al. [24].

The MSDM is based on the statistical difference of the average amplitude curves to measure the perceptual difference of two meshes. The average curvatures ($\mathrm{CM}_{\mathrm{si}}$) are calculated for each as the average of the minimum and maximum curvatures:

$$\mathrm{CMsi} = \frac{(\mathrm{CM}_{\mathrm{si}}) = |Cmin, si| + |Cmax, si|}{2} \tag{2}$$

The amplitude of minimum and maximum curvatures ($|Cmin, si|$ and $|Cmax, si|$) are deducted from the fair values of the curvature tensor. The approximation of the curvature tensor used, is that introduced by Cohen-Steiner et al. on spatial vicinity defined by the geodesic disc resulting from the projection of a sphere of radius h on the surface of mesh. The average and standard deviation of the average curvature in a spatial window w containing n peaks, denoted respectively μ_w *and* σ_w are defined as:

$$\mu_w = \frac{1}{n}\sum\nolimits_{si\in w} CMsi, \tag{3}$$

$$\sigma_w = \sqrt{\frac{1}{n}\sum\nolimits_{si\in w} (CMsi - \mu_w)^2}, \tag{4}$$

The covariance between the curvatures of two window s $w1$ *and* $w2$ of the compared meshes M1 and M2 is defined as:

$$\sigma_{w_1 w_2} = \frac{\sigma^{w_1}_{w_1 w_2} + \sigma^{w_2}_{w_1 w_2}}{2} \tag{5}$$

where $\sigma^{w_1}_{w_1 w_2}$ defines the covariance calculated on the window $w1$:

$$\sigma^{w_1}_{w_1 w_2} = \frac{1}{n} \sum\nolimits_{S_{1i} \in w_1} \left(\left(CM^{w_1}_{S_{1i}} \right) - \mu_{w_1} \right) \left(\left(CM^{w_2}_{S2i} \right) - \mu_{w_2} \right) \tag{6}$$

where $S2i$ is the nearest summit to $S1i$ on $S1i$ the covariance σ^{w2}_{w1w2} on the window w_2 is calculated in the same way. To calculate the overall distance between two meshes, MSDM based on local distances, we note MSDML:

$$MSDML = (\alpha * L(s)^a + \beta * C(s)^a + \gamma * M(s)^a)^{\frac{1}{a}} \tag{7}$$

With α, β, γ and a are scalars for combining different quantities. The parameters L, C, M represent respectively the differences bends, contrasts and structures measured by:

$$L(s) = \frac{||\mu_{w1} - \mu_{w2}||}{MAX(\mu_{w1}, \mu_{w2})} \tag{8}$$

$$\mathbf{C}(\mathbf{w1}, \mathbf{w2}) = \frac{||\boldsymbol{\sigma}_{\mathbf{w1}} - \boldsymbol{\sigma}_{\mathbf{w2}}||}{\mathbf{MAX}(\boldsymbol{\sigma}_{\mathbf{w1}}, \boldsymbol{\sigma}_{\mathbf{w2}})} \tag{9}$$

$$M(w1, w2) = \frac{||\sigma_{w1}\sigma_{w2} - \sigma_{w1}\sigma_{w2}||}{\sigma_{w1}\sigma_{w2}} \tag{10}$$

where w represents the number of local windows on mesh surfaces to compare, and a parameter that has the same value as in the Eq. 7. An improved version of MSDM named MSDM2 was proposed in 2011 by integrating a multi-scale analysis [29]. MSDM2 also compares two meshes that do not share the same connectivity through a matching step through the structure data AABB tree implemented in the CGAL [30]. We note that to establish a measure of perceptual symmetrical distance, MSDM2 calculates the average of the two distances unidirectional (respectively M_1 to M_2 and M_2 to M_1). MSDM and MSDM2 are based only on statistics of the curvatures magnitudes.

5.3.3 The Fast Mesh Perceptual Distance Metric

In 2012, a new metric for estimating the perceptual quality was introduced par Corsini et al. [31]. It is entitled Fast Mesh Perceptual Distance (FMPD). The type of this metric is reduced-reference, it is based on the comparison of overall roughness measurements calculated on the two grids to compare. The roughness descriptor retained in FMPD is

derived from Laplacian of the Gaussian curvature. For each summit *Si* the Gaussian curvature (noted CG_i) is established by the following equation:

$$CG_i = \left| 2\pi - \sum_{j \epsilon N_i(F)} \alpha_j \right| \tag{11}$$

or *Ni* (*F*) represents all vicinity facets at the summit *Si* and the j angle αj represent the crossing facet with the actual summit. The local roughness, calculated on a top *si* is approximated by the quantity:

$$RL_i = \left| CG_i + \frac{\sum_{j \in N_i(S)} D_{ij} CG_j}{D_{ii}} \right| \tag{12}$$

where $N_i(s)$ is the set of neighboring vertices aware summit, the matrix D it's the array of discrete Laplace established by:

$$D_{ij} = \frac{\cot(\beta_{ij}) + \cot(\beta_{ij})}{2} pourj \epsilon N_i(s) \tag{13}$$

$$D_{ii} = -\sum_j D_{ij} \tag{14}$$

where βij and $\beta ij'$ are the opposite angles in which the peak relies *si* to *sj*. Figures 4(b) and (d) represent respectively the color card of the roughness measurement on the surface of the Armadillo and Venus meshes. The warm colors match at high RL values, cold colors correspond to low values of RL. We note that this descriptor is able to properly evaluate and classify the surfaces of meshes into smooth and rough areas regions. FMPD in the local roughness measurements are modulated by a power function [32] to establish local values of roughness RLF_i in each peak s_i. This modulation is performed to capture the spatial masking effect on the mesh surfaces.

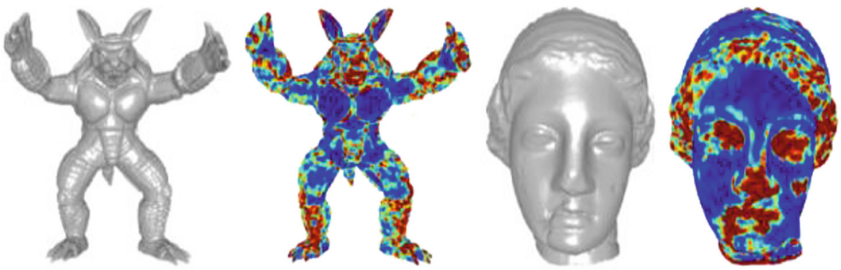

Fig. 4. (a) - and (c) - respectively present the 3D meshes of Armadillo and Venus, (b) - and (d) - present colors of the cards from the respective surfaces roughness Armadillo of mesh and mesh Venus.

The overall roughness is subsequently calculated by a steady sum of the local measurements:

$$\mathrm{RG} = \frac{\sum_i RLF_i a_i}{\sum_i a_i} \tag{15}$$

where a_i is a coefficient connected to the area of the incident facets at the summit s_i the measure of the perceptual distance FMPD is established as the difference between the values of global roughness RG_1 and RG_2 of two meshes M_1 and M_2 to compare:

$$FMPD = c|RG_1 - RG_2| \tag{16}$$

With c as a scalar set a scale parameter for the FMPD in the interval distances [0; 1].

5.3.4 The Dihedral Angle Mesh Error Metric

Recently, Vasa and Rus have developed a new metric of perceptual quality for static 3D mesh based on the dihedral angles [33]. This metric, named DAME (Dihedral Angle Mesh Error) offers a compromise between the complexity and the prediction efficiency. On each pair of triangles (t1 = $\{S_1S_2S_3\}$; t2 = $\{S_3S_2S_4\}$) neighbors of the mesh, the dihedral angle oriented are calculated use this expression:

$$D_{t1t2=\arccos(n1,n2)*sgn(n1.(s4-s3))} \tag{17}$$

where n_1 and n_2 represent respectively the surface normal associated with t1 and t2 triangles. Measurement of DAME perceptual distance is calculated as follows:

$$\mathrm{DAME} = \frac{1}{||\Omega||} \tag{18}$$

$$\sum\nolimits_{\{t1,t2\}\in\Omega} \left\| D_{t1t2} - \overline{D_{t2t2}} \right\| \cdot m_{t1t2}.(w_1 + w_2) \tag{19}$$

where D_{t1t2} and $\overline{D}_{t1t2}$ respectively represent the measurements of the dihedral angles of the two meshes to compare, m and w represent respectively a masking modeling function and a visibility coefficient.

6 Conclusion

In this paper, we have studied the importance of perceptual quality 3D meshes compared to the objective measures meshes. We have also enumerated the different existing approaches which are based on the metrics of the perceptual quality 3D meshes. We have also detailed various properties of the HVS, such as the CSF and the masking effect. It is important to consider these properties for guiding quality measures development process perceptual 3D meshes. These existing perceptual objective

metrics mainly considers the spatial masking effect to establish quality metrics collected for 3D meshes. Finally we have itemized metrics which are based on the HVS properties.

References

1. Lecuire, V., Duran-Faundez, C., Krommenacker, N.: Energy-efficient image transmission in sensor networks. Int. J. Sens. Netw. **4**(1/2), 37–47 (2008)
2. Salehpour, M., Behrad, A.: 3D face reconstruction by KLT feature extraction and model consistency match refining and growing. In: 2012 6th International Conference on Sciences of Electronics, Technologies of Information and Telecommunications (SETIT), Sousse, pp. 297–302 (2012)
3. Chan, A.T., Gamino, A.: Integration of assistive technologies into 3D simulations: an exploratory study. In: Information Technology: New Generations, Advances in Intelligent Systems and Computing, vol. 448, pp. 425–437. Springer (2016). ISBN 978-3-319-18295-7
4. El-Bendary, M.A.M., El-Tokhy, M., Kazemian, H.B.: Efficient image transmission over low-power IEEE802.15.1 network over correlated fading channels. In: The 6th International Conferences: Sciences of Electronics, Technologies of Information and Telecommunications "SETIT 2012", Mars 2012, Sousse-Tunisie, IEEE Conferences, pp. 563–567 (2012). doi:10.1109/SETIT.2012.6481973
5. Abderrahim, Z., Techini, E., Bouhlel, M.S.: State of the art: compression of 3D meshes. Int. J. Comput. Trends Technol. (IJCTT) **4**(6), 765–770 (2012)
6. Tang, H., Joshi, N., Kapoor, A.: Learning a blind measure of perceptual image quality. In: Proceedings of the 2011 IEEE Conference on Computer Vision and Pattern Recognition, pp. 305–312 (2011)
7. Hemanth, D.J., Balas, V.E., Anitha, J.: Hybrid neuro-fuzzy approaches for abnormality detection in retinal images. In: Proceedings of the 6th International Workshop Soft Computing Applications, SOFA 2014, Timisoara, Romania, 24–26 July 2014, pp. 295–305 (2014)
8. El-Bendary, M.A.M., El-Tokhy, M., Shawki, F., Abd-El-Samie, F.E.: Studying the throughput efficiency of JPEG image transmission over mobile IEEE 802.15.1 network using EDR packets. In: The 6th International Conferences: Sciences of Electronics, Technologies of Information and Telecommunications "SETIT 2012", Mars 2012, Sousse-Tunisie, IEEE Conferences, pp. 573–577 (2012). doi:10.1109/SETIT.2012.6481975
9. Escribano-Barreno, J., García-Muñoz, J.: Integrated metrics handling in open source software quality management platforms. In: Information Technology: New Generations. Advances in Intelligent Systems and Computing, vol. 448, pp. 509–518. Springer (2016). ISBN 978-3-319-18295-7
10. Triki, N., Kallel, M., Bouhlel, M.S.: Imaging and HMI, fondations and complementarities. In: The 6th International Conferences: Sciences of Electronics, Technologies of Information and Telecommunications, SETIT 2012, Mars 2012, Sousse-Tunisie, IEEE Conferences, pp. 25–29 (2012). doi:10.1109/SETIT.2012.6481884
11. Nandi, D., Ashour, A.S., Samanta, S., Chakraborty, S., Salem, M.A., Dey, N.: Principal component analysis in medical image processing: a study. Int. J. Image Min. **1**(1), 65–86 (2015)
12. Cho, J.-W., Prost, R., Jung, H.-Y.: An oblivious watermarking for 3-D polygonal meshes using distribution of vertex norms. IEEE Trans. Sig. Process. **55**(1), 142–155 (2007)

13. Wang, K., Lavoué, G., Denis, F., Baskurt, A.: Robustand blind mesh watermarking based on volume moments. Comput. Graph. **35**(1), 1–19 (2011)
14. Abderrahim, Z., Techini, E., Bouhlel, M.S.: Progressive compression of 3D objects with an adaptive quantization. Int. J. Comput. Sci. Issues (IJCSI) **10**(2), 504–511 (2013)
15. Campbell, F.-W., Robson, J.-G.: Application of Fourier analysis to the visibility of gratings. J. Physiol. **197**, 551–566 (1968)
16. Hirai, K., Tsumura, N., Nakaguchi, T., Miyake, Y., Tominaga, S.: Spatio-velocity contrast sensitivity functions and video quality assessment. In: International Symposium on Intelligent Signal Processing and Communication Systems, pp. 1–4 (2010)
17. Ninassi, A., Meur, O.L., Le Callet, P., Barba, D.: On the performance of human visual system based image quality assessment metric using wavelet Domain. In: Proceedings of the SPIE Human Vision and Electronic Imaging (2008)
18. Ninassi, A., Meur, O.L., Le Callet, P., Barba, D.: Which semi-local visual masking model for wavelet based image quality metric In: Proceedings of IEEE International Conference on Image Processing, pp. 1180–1183 (2008)
19. Fernandez-Maloigne, C., Larabi, M.-C., Bringier, B., Richard, N.: Spatio temporal characteristics of the human color perception for digital quality assessment. In: Proceedings of International Symposium on Signals, Circuits and Systems, pp. 203–206 (2005)
20. Kelly, D.-H.: Visual contrast sensitivity. Opt. Acta: Int. J. Opt. **24**(2), 107–129 (1977)
21. Daly, S.-J.: Engineering observations from spatio velocity and spatio temporal visual models. In: Proceedings of the SPIE Human Vision and Electronic Imaging III, vol. 3299, pp. 180–191 (1998)
22. Wang, Z., Bovik, A.-C.: Modern Image Quality Assessment. Morgan & Claypool, San Rafael (2006)
23. Rogowitz, B.-E., Rushmeier, H.-E.: Are image quality metrics adequate to evaluate the quality of geometric objects. In: Proceedings of SPIE Human Vision and Electronic Imaging, pp. 340–348 (2001)
24. Corsini, M., Drelie Gelasca, E., Ebrahimi, T., Barni, M.: Watermarked 3-D mesh quality assessment. IEEE Trans. Multimedia **9**(2), 247–256 (2007)
25. Lavoué, G.: A multiscale metric for 3D mesh visual quality assessment. Comput. Graph. Forum **30**(5), 1427–1437 (2011)
26. Lavoué, G., Drelie Gelasca, E., Dupont, F., Baskurt, A., Ebrahimi, T.: Perceptually driven 3D distance metrics with application to watermarking. In: Proceedings of SPIE Electronic Imaging (2006)
27. Wang, Z., Bovik, A.-C., Sheikh, H.R., Simoncelli, E.P.: Image quality assessment: from error visibility to structural similarity. IEEE Trans. Image Process. **13**(4), 600–612 (2004)
28. Alliez, P., Tayeb, S., Wormser, C.: 3D fast intersection and distance computation (AABB tree). In: CGAL User and Reference Manual (2012)
29. Wu, J.-H., Hu, S.-M., Tai, C.-L., Sun, J.-G.: An effective feature-preserving mesh simplification scheme based on face constriction. In: Pacific Conference on Computer Graphics and Applications, pp. 12–21 (2001)
30. Gelasca, E.-D., Ebrahimi, T.: Objective evaluation of the perceptual quality of 3D watermarking. In: IEEE International Conference on Image Processing, pp. 241–244 (2005)
31. Corsini, M., Gelasca, E.-D., Ebrahimi, T.: A multi-scale roughness metric for 3D watermarking quality assessment. In: Workshop on Image Analysis for Multimedia Interactive Services (2005)
32. Wang, K., Torkhani, F., Montanvert, A.: A fast roughness-based approach to the assessment of 3D mesh visual quality. Comput. Graph. **36**(7), 808–818 (2012)
33. Vása, L., Rus, J.: Dihedral angle mesh error: a fast perception correlated distortion measure for fixed connectivity triangle meshes. Comput. Graph. Forum **31**(5), 1715–1724 (2012)